Biosensors and Bioelectronics 138 (2019) 111314

Contents lists available at ScienceDirect

Biosensors and Bioelectronics

journal homepage: www.elsevier.com/locate/bios

FÖrster resonance energy transfer (FRET)-based biosensors for biological applications

Xiaojing Zhang, Yue Hu, Xiaotong Yang, Yingying Tang, Shuying Han, An Kang, Haishan Deng, Yumei Chi, Dong Zhu*, Yin Lu**

Jiangsu Key Laboratory for Pharmacology and Safety Evaluation of Chinese Materia Medica, School of Pharmacy, Nanjing University of Chinese Medicine, Nanjing, Jiangsu, 210023, PR China

ARTICLE INFO

Keywords:
Fluorescent biosensor
FRET
Nanomaterials
Multi-FRET
Nanomedicine

ABSTRACT

FÖrster resonance energy transfer (FRET)-based biosensors have achieved great success for biological applications. However, what is not extensively appreciated is the growing role as versatile FRET biosensors within a similar biological context. This review provides a brief introduction of recent advances in principle, the designing strategies and kinds of applications of FRET biosensors. For each FRET biosensor, the appropriate background and fabrication is explained before studying their related applications. The prominent roles of nanomaterials are present in the development of more sensitive and specific FRET biosensors. Finally, the challenges and outlooks of FRET biosensors are emphasized.

1. Introduction

Fluorescent technology (Albert et al., 2000; Zhu et al., 2018; Thevenot et al., 1999) has been extensively used in medical diagnosis (Yue et al., 2018), food safety (Xu et al., 2014), and environmental monitoring (Lu et al., 2017) because of its inherent sensitivity and high selectivity (Liu et al., 2018). However, although plenty of fluorescent biosensors have been employed for kinds of applications, they are still unsatisfactory to accurately quantitate because fluorescent signal is easily interference by many factors especially for the surrounding environment (pH and temperature) and fluorimeter (slight change of excitation or emission intensity) (Samanta et al., 2018; Mehrotra et al., 2016). To overcome the problem, the ratiometric fluorescent biosensor has been developed to quantitate the targets by the ratio of the simultaneously recording fluorescence intensity at two wavelengths (Thevenot et al., 2001; Medintz et al., 2003; Wang et al., 2018; Morris et al., 2010). The ratiometric fluorescent strategies include intra-molecular charge transfer (ICT) (Du et al., 2018; Sun et al., 2017) and FÖrster resonance energy transfer-based approach (Kikuchi et al., 2004; Feng et al., 2018; Zhao et al., 2015). For ICT, two factors usually interfere the accuracy of biosensors: 1) Binding of the targets could promote or inhibit ICT interactions to induce into remarkable shifts of the sensors absorption maxima. 2) Relatively broad fluorescence spectrum makes it difficult to accurately determine the ratio of the two fluorescence peaks. FRET can partly solve the problem because the single excitation in FRET can result in a longer emission (Zhang et al., 2008; Hu et al., 2014; Hu et al., 2013). Table 1 compares these technologies used in fluorescent biosensors.

By producing a non-invasive, real-time fluorescence signal changing with the spatial and temporal distributions of the fluorescent substance (Luby et al., 2016; Charron et al., 2018; Zhu et al., 2016), FRET has been served as the designing strategy of different biosensors for the diagnosis of disease, drug screening, and other biological applications. Besides of the high sensitivity, specificity and fast responsibility, FRET-based biosensors also have the unique advantages such as simplicity and homogeneous assay without any washing, which can be beneficial to perform accurate quantitative measurement *in vitro* and in living cells (Kikuchi et al., 2004; Zhu et al., 2016; Klymchenko, 2017; Li et al., 2017; Yuan et al., 2013, 2015; Albers et al., 2006; Chen et al., 2015).

This review focuses on the biosensors relying on FRET strategies for the detection of small-molecular or biological macromolecular *in vitro*, living cells and *in vivo*. The principles of these FRET biosensors are covered, followed by kinds of applications. Moreover, we present the prominent roles of nanomaterials in the development of more sensitive and specific FRET biosensors. Finally, we also emphasized on the challenges and outlooks of FRET biosensors.

* Corresponding author.
** Corresponding author.
E-mail addresses: dongzhu@njucm.edu.cn (D. Zhu), luyingreen@126.com (Y. Lu).

https://doi.org/10.1016/j.bios.2019.05.019
Received 10 April 2019; Accepted 8 May 2019
Available online 10 May 2019
0956-5663/

Table 1
Comparision of commonly used fluorescence biosensors.

Development of Strategy		Disadvantages	Advantages	Ref.
Direct fluorescent biosensor	ICT-based biosensor	High-background	Quantitation; Semiquantitative;Cellular imaging;	(Albert et al., 2000; Yue et al., 2018; Xu et al., 2014; Lu et al., 2017)
Ratiometric fluorescent biosenosor		Serious interference	Imaging; Accurate quantitation	(Kikuchi et al., 2004; Feng et al., 2018)
	FRET-based biosensor	Low-FRET efficiency	Ratiometric Imaging; Accurate quantitation	(Luby et al., 2016; Charron et al., 2018; Wang et al., 2012)

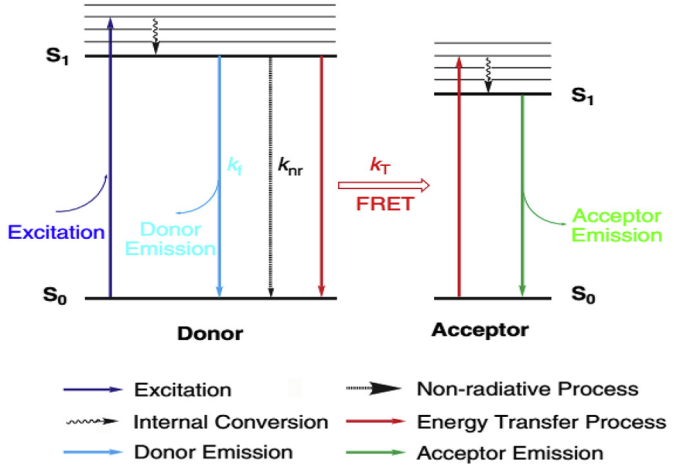

Fig. 1. Basic principle of FRET. Reprinted (adapted) with permission from Kikuchi et al. (2004).

2. FRET biosensor

2.1. Principle of FRET

FRET is an energy transfer process between a pair of light-sensitive molecules, where the donor fluorophore, initially in its electronic excited state, transfers energy to an acceptor chromophore as shown in Fig. 1 (Lakowicz, 1991; Gadella, 2009; Sun et al., 2010).

The FRET efficiency (E) depends on multiple factors that are summarized as 1) the spectral overlap (*J*) of the donor emission spectrum and the acceptor absorption spectrum, 2) the distance between the donor and the acceptor (typically in the range of 1–10 nm), and 3) the relative orientation of the donor emission dipole moment and the acceptor absorption dipole moment. In the traditional FRET, one donor (D) could combine with one acceptor (A). For such the single pair of fluorophores, the efficiency (E) of FRET is inversely proportional to the sixth power of the distance between donor and acceptor, making FRET extremely sensitive to small changes in distance (r) between the donor and the acceptor. Recently, a large number of biosensors based on nanomaterials have been designed. In nanomaterial-based FRET, some studies provided a theoretical model for the FRET (Berney and Danuser, 2003; Clapp et al., 2004; Corry et al., 2005; Raicu, 2007; Hildebrandt et al., 2017), which includes two cases of any As-D couple (n_a) where single donor (D) attached multiple acceptor (As), or any Ds-A couple (n_d) where single acceptor (A) can bond with multiple donors (Ds). As shown in equation (1), *E* can be expressed as follow by using r and R_0:

$$E = \sum_{i=1}^{n_d} \left[\frac{R_0^{\,6 \sum_{j=1}^{n_a} \frac{1}{r_{ij}^6}}}{1 + R_0^6 \sum_{j=1}^{n_a} \frac{1}{r_{ij}^6}} \right] \frac{1}{n_d} \tag{1}$$

In Eq. (1), R_0 is the Förster distance of this pair of donor and acceptor, i.e. the distance at which the energy transfer efficiency is 50%, r_{ij} is the distance from the donor to the acceptor. Thus energy transfer was dependent on the distance between donor and acceptor.

Normally, R_0 could be 2–10 nm (nm) for commonly used fluorophores and relied on *J* and donor quantum yield (Φ):

$$R_0 = 0.0211(J\Phi k^2 n^{-4})^{1/6} \tag{2}$$

In Eq. (2), k^2 is the orientation of the donor and acceptor transition dipole moments, *n* is the refractive index of medium between the FRET pairs. Thus, a pair of FRET fluorophore with large spectral overlap were necessary. And the change of distance (*r*) between the donor and the acceptor acts as off/on the switch of FRET.

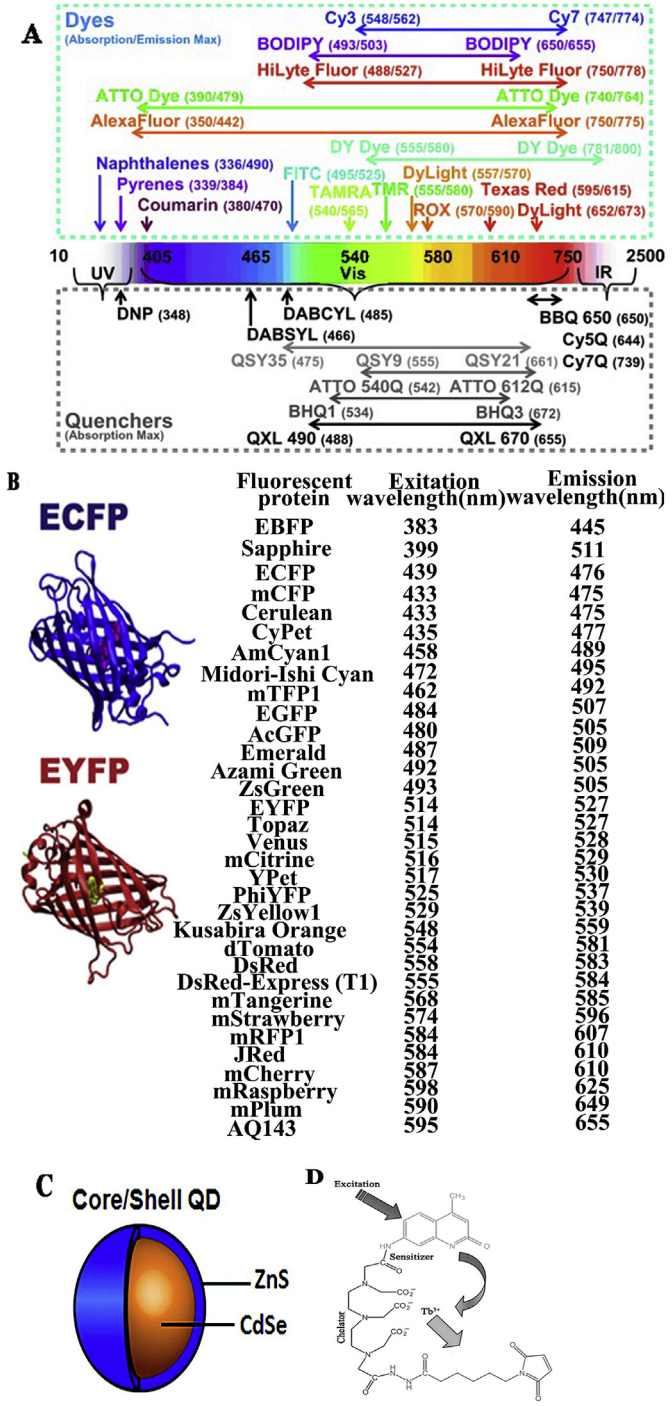

Fluorescent protein	Exitation wavelength(nm)	Emission wavelength(nm)
EBFP	383	445
Sapphire	399	511
ECFP	439	476
mCFP	433	475
Cerulean	433	475
CyPet	435	477
AmCyan1	458	489
Midori-Ishi Cyan	472	495
mTFP1	462	492
EGFP	484	507
AcGFP	480	505
Emerald	487	509
Azami Green	492	505
ZsGreen	493	505
EYFP	514	527
Topaz	514	527
Venus	515	528
mCitrine	516	529
YPet	517	530
PhiYFP	525	537
ZsYellow1	529	539
Kusabira Orange	548	559
dTomato	554	581
DsRed	558	583
DsRed-Express (T1)	555	584
mTangerine	568	585
mStrawberry	574	596
mRFP1	584	607
JRed	584	610
mCherry	587	610
mRaspberry	598	625
mPlum	590	649
AQ143	595	655

Fig. 2. (A) Absorbance and emission maxima of common available fluorescent dye and quencher families. Reprinted (adapted) with permission from Sapsford et al. (2006). (B) Simplified structure of fluorescent proteins, ECFP and FYFP and lists of commonly used fluorescent proteins. Reprinted (adapted) with permission from Kyrychenko et al. (2017). (C) Cartoon structure of a CdSe/ZnS QD. Reprinted (adapted) with permission from Russ Algar et al. (2011). (D) Structure of the Tb probe. Reprinted (adapted) with permission fromSapsford et al. (2006).

2.2. Introduction of donor and acceptor

Most commercial fluorophores can be available as FRET donors or acceptors as shown in Fig. 2. The organic donors covered ultraviolet (UV) dyes such as coumarin-, naphthalene-, and pyrene-based analogue, and near-infrared (NIR) dyes, including cyanine- (Cy3.5, Cy5.5), rhodamine. Some organic molecules were loaded or conjugated into the functionalized polymeric microspheres or onto their surface (by using functionalized groups such as biotin, avidin, amines, sulfates, and carboxylates) to increase the fluorescent signal for targets, or were modified to increase the water-solubility (Horvath et al., 2005; Zahavy et al., 2003). On the other hand, the modified fluorophores were also combined with the shell or nanoparticles (NPs) to obtain strong fluorescence (Balzani et al., 2000; Vicinelli et al., 2002; Kaafarani et al., 2003). Quenchers as the FRET acceptors are increasingly prevalent due to their wide absorption spectrum and high extinction coefficient (Maxwell et al., 2002), which included many of organics such as 4-(4′-dimethylaminophenylazo) benzoic acid (Dabcyl) and 4-dimethylaminoazobenzene-4′-sulfonyl (Dabsyl), two of ordinary non-fluorescence acceptors, QSY9, QXL, ATTO dyes, blackberry, and black hole families (BHQ-3, BHQ-5), and metallic materials for instance gold nanoparticles due to broad absorption spectra (Sapsford et al., 2006).

Fluorescent proteins (FPs) (Fig. 2B) such as CFP, GFP, BFP and YFP have also been served as the critical players of the donor or acceptor for monitoring the protein-protein interactions or conformational changes of individual proteins in living cells (He et al., 2004; Rehm et al., 2002; Periasamy, 2001; Enterina et al., 2015; Kyrychenko et al., 2017). Besides, lanthanides cations such as terbium and europium (Fig. 2D) as long-lifetime dyes, have emerged as the prominent role of time-resolved FRET system (Selvin, 2005; Pulli et al., 2002; Qin et al., 2003). Moreover, fluorescent nanoparticles including quantum dots (QDs) (Fig. 2C) and carbon dots (CDs) with broad absorption, can serve as both donor and acceptor (Sidhu et al., 2017; Russ Algar et al., 2011). The structure of linker space and property of fluorophore pair could also affect the intrinsic FRET efficiency of the probe (Mccartney et al., 2017).

2.2.1. Fabrication of FRET-based biosensor

Multiple kinds of FRET biosensors are designed as shown in Table 2. Commonly used FRET biosensor was fabricated by a pair of donor and acceptor with a close position, and a specify receptor (such as protein, DNA) was used to identify the target. The structure of the biosensor is sandwiched between the donor and the acceptor (Peroza et al., 2015; Mohsin et al., 2014). After binding of receptor with the targets, FRET signal is observed due to the destruction of the pair of donor and acceptor because of the conformation change or the cleavage of the receptor. It has been utilized for quantifying analysis of targets such as ions, proteins and nucleic acid *in vitro* or in living cells (Klymchenko, 2017; Li et al., 2015). For whole-animal imaging by *in vivo* microscopy, many FRET biosensors were limited due to the attenuation of the fluorescence and absorption of the tissue for visible light (Leeuwen et al., 2015). And the ideal fluorophores for animal imaging should have emissions at the NIR region (> 700 nm), where the absorption, light-attenuation, and auto-fluorescence are minimum (Guo et al., 2013; Luo et al., 2011; Kobayashi et al., 2010).

Recently, a dual-FRET biosensor was successfully fabricated for the sequential sensing of MMP-2 and caspase-3 via a dual-stage turn-on fluorescence processes (Li et al., 2015). The biosensor was comprised of 5 (6)-carboxyfluorescein (FAM) as donor and two 4-{[4-(dimethylamino)-phenyl]-azo}-benzoic acid (Dabcyl) moieties as FRET quench fluorophore pairs. While, MMP-2 specific peptide sequence and caspase-3 sensitive peptide unit were utilized as cleavable substrates between the dual-FRET pairs, respectively. In addition, a multi-step FRET biosensor was used to study molecular interaction beyond 1–10 nm through the energy transfer by an FRET antenna (Saha et al., 2016), and which would expand the application of FRET biosensor in biology research. In this biosensor, energy transfer from pyrene (Py) to rhodamine B (RhB) occurred in two steps-(i) firstly from Py to Acriflavine (Acf) and (ii) secondly Acf transfer this energy to RhB. Also direct energy transfer from Py to RhB may become significant in presence of Acf.

On the other hand, some peculiar nanostructures such as mesoporous silica nanoparticles (MSNs), liposomes, polymer micelles, scaffolds and nanoemulsions were also utilized as FRET-based biosensors

Table 2
Multiple FRET-based biosensors.

Description	Measuring parameter	Feature	Application	Ref.
Traditional FRET biosensor	Ratio of fluorescent intensity	a pair of donor and acceptor with the distance of 1–10 nm	Detection of the conformation; ions, proteins and nucleic acid *in vitro* and in living cells	(Peroza et al., 2015; Mohsin and Ahmad, 2014)
dual-FRET biosensor		a fluorophore and two quenchers with the distance of 1–10 nm	one on-going pathology	(Li et al., 2015; Leeuwen et al., 2015)
multi-step FRET sensor peculiar nanostructures for FRET sensor with signal enhancement		molecular effect beyond 1–10 nm A nanocarrier system	research among molecular interaction tracking drug from subcellular to whole-animal; a non-invasive ways	Saha et al. (2016) (Toy et al., 2014; Smith and Gambhir et al., 2017; Petersen et al., 2012)

for signal enhancement due to their low toxicity and the improvement of energy transfer efficiency (Bremer et al., 2001; Torchilin et al., 2005; Webster, 2006; Park et al., 2009; Yan et al., 2013; Li et al., 2013; Wang et al., 2016; Pelaz et al., 2017; Lane et al., 20015). For example, MSNs possess excellent capacity for cargo loading due to stable mesoporous structures, large surface area, tunable pore sizes, and well-defined surfaces. The fluorophores of FRET pairs were simultaneously encapsulated in the inner or combined onto the surface of MSN to increase the fluorescence signal, obtain lower detection limits, and preserve the function of the targets (Charron and Zheng, 2018; Thapaliya et al., 2015). Other various integrated FRET biosensors have also been achieved for the applications in real-time imaging, theranostics and sensing with a non-invasive way in living cells or animal (Kunjachan et al., 2015; Toy et al., 2014; Smith and Gambhir, 2017; Petersen e t al., 2012; Mura et al., 2012; Zheng et al., 2015; Charron et al., 2015; Mirkin et al., 2015; Chen et al., 2017; Chen et al., 2016; Ekdawi et al., 2015). By using these FRET biosensors, the micro-distribution and subcellular localisation of nanosensor in ex vivo tissue sections is also becoming feasible (Ekdawi et al., 2015). These FRET biosensors provide the advantages of tracking nanomedicine from subcellular to whole-animal due to its sensitivity and accessibility (James and Gambhir, 2012; Priem et al., 2015; Pansare et al., 2012; Yao et al., 2014; Merian et al., 2012).

2.2.2. Analysis of FRET data

FRET is usually detected by appropriately equipped fluorescence spectrometer or microscopes, either as a decrease in the fluorescence intensity, lifetime, or anisotropy of the donor, or as an increase in the fluorescence intensity of the acceptor upon donor excitation (if the acceptor is fluorescent), or as a combination of these two effects. A FRET ratio of A/D was introduced as a variable in the FRET signal that corresponds to the amount of targets, where A and D respectively represent the maximal fluorescent intensity of the acceptor and donor (Zhou et al., 2012; Torchilin, 2014). The crosstalk of spectrum between the donor and acceptor is a major challenge for quantitative FRET analysis. The donor emission can overlap with the acceptor emission, and the acceptor may also be directly excited at the donor excitation wavelength. Multiple efforts have been attempted to overcome these challenges. Fluorophores exhibiting a large Stokes shift, such as quantum dots and upconversion nanocrystals, have been used to reduce the crosstalk. Moreover, time-resolved FRET assays with fluorophores that exhibit long half-lives, such as lanthanide chelate dyes, have proven effective in eliminating interfering fluorescence. Liao group developed a method to mathematically analyze the spectrum crosstalk between the FRET donor and acceptor by introducing a second excitation (Liao et al., 2015). In this assay, an emission wavelength at which only the donor emits is used to calculate donor emission at the acceptor emission wavelength, and a second excitation wavelength at which only the acceptor emits is used to calculate the acceptor direction emission. Jin et al. provides a unique combination of correction performance parameters by careful implementation of several spectroscopy technologies (time-resolved fluorescence detection, color multiplexing, biospectral crosstalk correction) into a FRET nucleic acid assay (Jin et al., 2015). Chen et al. also developed a correct approach to quantitatively analyze the FRET emission (Chen et al., 2007). Three filter tubes are utilized to collect fluorescence images of the donor emission at the donor excitation, the acceptor emission at the donor excitation, and the acceptor emission at the acceptor excitation. These collected signal intensities are then expressed as functions of four crosstalk parameters and three fluorescence components: donor fluorescence, sensitized acceptor FRET emission, and the direct emission of acceptor. The crosstalk parameters were determined from samples with only donor or acceptor, and the three fluorescence components were calculated by a three-variable linear equation group. Although these approaches greatly reduce spectrum crosstalk in the FRET assay and simplify FRET signal analysis, more generalized approaches are needed.

The fluorescent imaging based on FRET can give spatial data and

Table 3
Summary of recent applications of FRET-based biosensor.

Analyte	Fluorophore	Receptor-Linker	Ways	LOD/liner range	Ref.
Small molecules					
NO	Atto620/Cy5	cytochrome *c* peroxidase	Content	10 nM	Strianese et al. (2010)
Zinc	CFP/YFP	Metallothioneins SmtA	Content	0.1 μM	Mohsin et al. (2015)
Immune molecules					
aflatoxin B_1	Red/Green emission QDs	Monoclonal anti-AFB_1	Content	0.1302pM	Xu et al. (2014)
Enzymes					
neutrophil elastase	YFP/CFP	a specific recognition sequence	Activity	na	Faccio and Salentinig (2017)
matrix metallopeptidase 9	5-FAM/QXL520	specific peptide substrate	Activity	na	Lee et al. (2018)
BSA/HSA	pyrimidine derivative	Schiff-base ligand	Conformational change of protein	na	Ghosh et al. (2018)
calpain	CFP/YFP	calpain cleavage sequence	Activity	na	Mccarttny et al. (2017)
MMP-2/caspase-3	FAM/Dabcyl	cleavable substrates of MMP-2 and caspase-3	Activity	Tumours ~ 1 cm in diameter	Kwon et al. (2017)
MMP-2/MMP-7	AMC/BCTOT-Eu^{II}	cleavable peptide spacer	Activity	na	Wang et al. (2012)
MT1 MMP	ECFP/R-PE	PEbody	enzymatic activity at the surface	na	Limsakul et al. (2018)
telomerase	fluorescein/BHQ	Loading with MSN	activity	na	Qian et al. (2013)
Nucleic acids					
DNA	Atto 488/Atto 647N	dye-labeled "imager"/complementary strands		~ 72 nM	Auer et al. (2017)
ochratoxin A	colloidal cerium oxide nanoparticles/GQDs	OTA aptamer (electrostatic assembly)	Content	2.5 pg mL^{-1}	Tian et al. (2017)
SYBR Green I	anthanide-doped NPs(UCNPs)/ssDNAs	coordination interaction		3.2 nM	Wu et al. (2018)
Tissues					
organs	Cy 5.5/Cy 7.5	encapsulation	Content	na	Bouchaala et al. (2016)
Thermal-responsives					
	FITC/Rhodamine B (RB)	PECT self-assembly	imaging	na	Huang et al. (2017)

optical information (Ray et al., 2014). FRET imaging could also obtain abundant visual information in regard to nanoparticle integrity, efficiency and behavior between the biosensors with proteins, or living cells. For FRET imaging, the semi-quantitative result was achieved by analyzing the ratio of corresponding pixel intensity at donor and acceptor channels *in cell* and *in vivo* (Zhang et al., 2018; Bouchaala et al., 2016).

3. Application of FRET-based biosensor

FRET plays significant role in designing various biosensors for the clinical, pharmaceutical, toxicological, or agri-food analysis among others (Jin et al., 2010; Xu et al., 2017; Limsaku et al., 2018; Ibraheem and Campbell, 2010; Tian et al., 2010; Saha et al., 2018; Barker et al., 1998). According to the analytes (in Table 3), the FRET biosensors can be classified including small molecules, antibodies (immune molecules), enzymes, nucleic acids, and tissue-based biosensors (Mehrotra, 2016; Mohsin et al., 2015; Goldsmith, 1975). Recently, FRET biosensors have also been successfully utilized for the detection of compounds, *in vivo* imaging, drug delivery, and image-guided surgery (Shen et al., 2014; Rai et al., 2015; Zhang et al., 2006).

3.1. Small molecule FRET biosensors

FRET biosensors have been utilized for detection of many small molecules such as nitric oxide (NO), metal ions and other organic small molecules (Tian et al., 2010; Saha et al., 2018). NO plays an important role in multitudinous biological functions such as the carcinogenic and neurodegenerative disorders (Culotta and Koshland, 1992). A fast and reversible fiber-optic NO-selective fluorescent biosensor was successfully developed with a detection limit of 20 μM and linear up to 1 mM NO by immobilizing the Cytochrome *C* at end of optical fiber in polyacrylamide-matrix or covalent binding to the gold nanobeads (Barker et al., 1998). After that, Maria Strianese designed a NO-sensitive FRET sensor, where cytochrome *c* peroxidase (CcP Ex = 645 nm) was labeled by a fluorophore (Em = 645 nm) as shown in Fig. 3A. A FRET was occurred by the energy transfer from the labeled fluorophore (Atto620 or Cy5) to the protein NO-free labeled cytochrome *c* peroxidase (CcP) (Strianese et al., 2010). At the presence of NO, the CcP exhibited a disappearance of absorption spectrum at 645 nm ascribed to the conformational changes of CcP after the binding with NO, resulting in the renewing of the fluorescence. The biosensor showed a lower detection limit of 10 nM compared to the previous work (Barker et al., 1998), demonstrating FRET biosensor can be used for the detection of extremely low NO level. Other than NO, Mohd. Mohsin reported a fluorescent protein-based biosensor for the detection of Zinc *in vitro*, in living cells and microorganisms (Mohsin et al., 2015). In the FRET pair, CFP (Em 485 nm) and YFP (Em 535 nm), was covalently linked to the two flank, N- and C- terminus of signal peptide of Metallothioneins SmtA, a cysteine-rich protein in *Cyanobacterium Synechococcus* sp. The FRET signal was increased significantly with the increase of zinc concentration, providing a linear detection range for Zn quantification between 5.0 μM and 2.0 mM, which is consistent with previous report (Duncan et al., 2006).

3.2. FRET immunosensors

In addition to small molecules, FRET biosensors have also been applied for the detection of immune molecules (Goldsmith, 1975; Haab, 2003; Zhu et al.,2010, 2014, 2015; Lai et al., 2013; Lequin, 2005). And the FRET biosensors were mostly linked via -SiOCN/-NH_2, –COOH/-NH_2, and biotin/strepatividin (Kumar et al., 2009; Wang et al., 2014; Wang et al., 2014, 2014; Song et al., 2012; Zhang et al., 2011). Their fabrications are various as demonstrated in Fig. 3C. Compared to standard enzyme-links or fluorescent sandwich immunoassays, FRET-based immunosensors have unique merits of free operation of washing

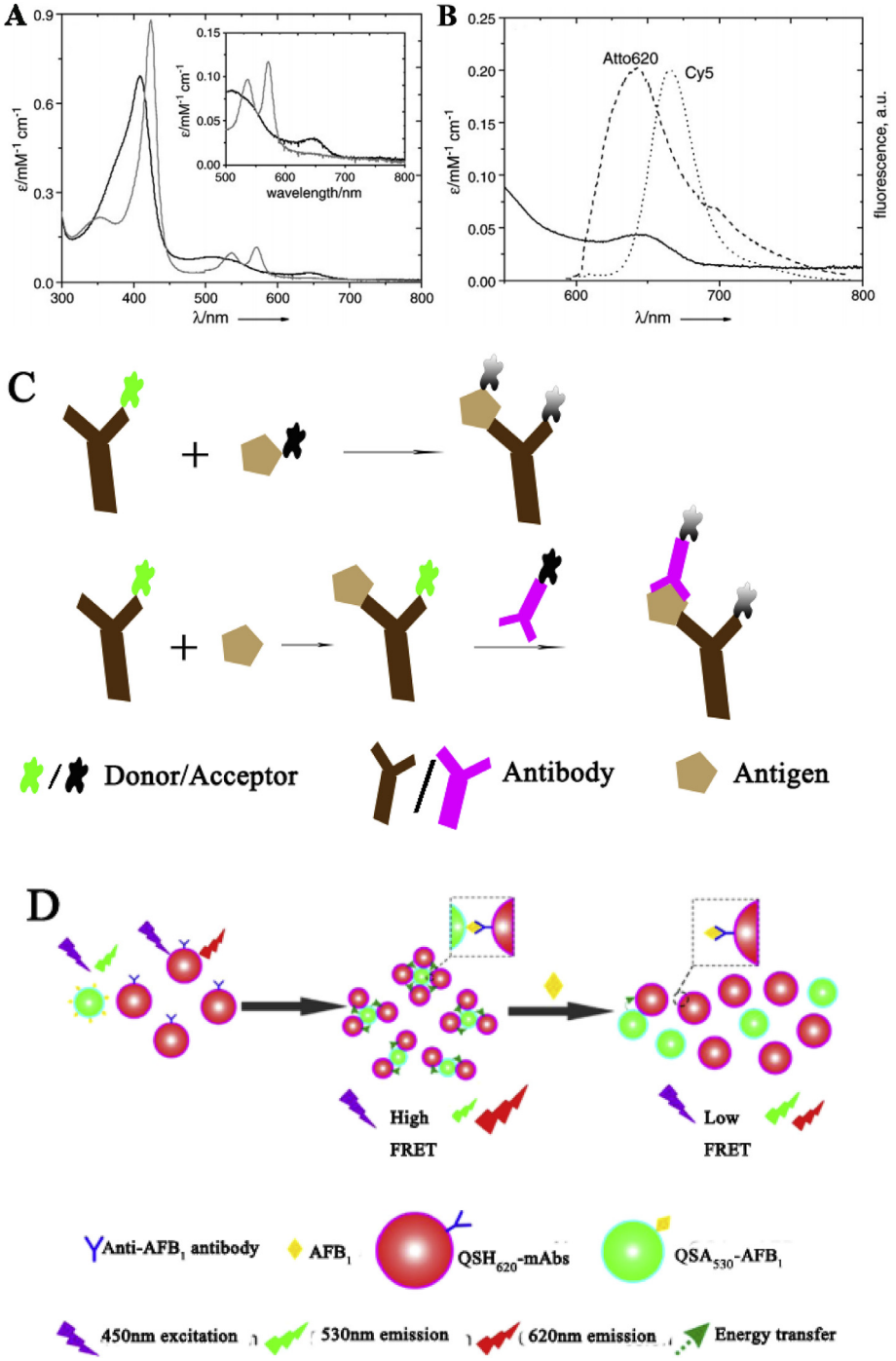

Fig. 3. (A) Absorption spectrum of NO-free (black) and NO-bound (grey) CcP. (B) Absorption spectrum of NO-free CcP (solid line) and emission spectra of Cy 5 (dotted line) and Atto 620 (dashed line). Reprinted (adapted) with permission from Strianese et al. (2010). (C) Commonly used FRET-based biosensor consisted of antibody and antigen. (D) Schematic structure of FRET-based immunosensor for the sensitive detection of AFB1. Reprinted (adapted) with permission from Xu et al. (2014).

and separation steps, excellent stability, specificity and ratiometric measurement (Hildebrandt et al., 2017; Haab et al., 2003). A great amount of FRET-based immunoassays had been successfully developed (Xu et al., 2014; Knopp, 2006).

Kattke et al. designed a FRET biosensor for the detection of mold spores in solution (Kattke et al., 2011). They conjugated fluorescent QDs to antibodies, which were then mixed with a solution of spores labeled with a quencher. The fluorescence was recovered upon addition of unlabeled spores in a dose-dependent manner, owing to the displacement of the QD-antibody conjugates from the quencher-spores. This FRET biosensor enabled detection of spores doses as low as 103 spores/mL. Stinger et al. proposed a FRET biosensor for the detection of antigen based on the conformational changes upon binding to the antigen (Stringer et al., 2008). They first conjugated protein A onto the surface of QDs, which enabled the oriented assembly of a dye-labeled IgG antibody against the Troponin I protein, resulting in FRET between the QD and dyes on the antibody. The assay could obtain a limit of detection (LOD) of the 200 nM. Xu reported a FRET-based immunosensor for the sensitive detection of aflatoxin B_1 (AFB_1) with a LOD of 0.13 pM (0.04 ng/ml) in rice grains using different-sized QDs

(Xu et al., 2014). As shown in Fig. 3D, to avoid potential irregular aggregation between two kinds of QDs, monovalent monoclonal antibody (mAb)-labeled red QDs (~0.84 anti-AFB1 mAbs per QD) and multivalent hapten-labeled green QDs (~6.8 AFB1 per QD) were utilized as acceptor and donor, respectively. The interactions of anti-AFB1 mAbs and AFB1 promoted one or more acceptors bound with a multivalent AFB1-labeled donor, resulting in energy transfer from the green QDs to the red QDs. This sensor performed a linearity with concentration range of 0.19–16 pM, indicating the FRET can be a promising method for AFB_1 in food safety at a low concentration (Xu et al., 2014).

3.3. Enzymatic FRET biosensors

The FRET biosensors are expansively exploited for the detection of biomarkers and enzymatic activities *in vitro* and in/on the surface of living cells (Zadran et al., 2012; Cao et al., 2007; Lee et al., 2018). Commonly, the FRET biosensors were designed for the detection of proteins dependent upon two elements, a pair of donor-acceptor and a specific recognition module for the targets (Fommer et al., 2009; Mertens et al., 2012; Kikhney et al., 2015). A conformational change of the targets results in the switch of "turn on/off" of FRET. Greta Faccio et al. fabricated a FRET-based biosensor for the detection of neutrophil elastase (NE) activity (Faccio et al., 2017). As shown in Fig. 4A, YFP and CFP was covalently combined with the linker, which has a specific recognition sequence for NE that belongs to a relevance inflammatory serine protease. Ghosh also designed a biosensor based on FRET by utilizing the synthesized pyrimidine derivative as fluorescent probe in Fig. 4B (Ghosh et al., 2018). A kind of pyrimidine based Schiff-base ligand, 2-(2-(Anthracen-9-ylmethylene) hydrazinyl)-4-,6-dimethyl pyrimidine (ANHP), was used to ascertain the conformational change of protein, and the FRET biosensor showed high sensitivity.

Sidhu designed a highly selective biotin-CDs-naphthalimide biosensor for monitoring the activity of thioredoxin reductase (TrxR) in cancer cell and pharmacological screening of cancer (Sidhu et al., 2017). As shown in Fig. 4C, a FRET platform was prepared by conjugating naphthalimide onto the surface of CDs through a disulfide linkage, which obtained a limit of detection of 7.2×10^{-8} M TrxR. Similarly, Lee fabricated an enzymatic-sensitive inkjet printing FRET biosensor for high-throughput screening assay against MMP-9 using 5-FAM as a fluorescent donor and QXL520 as a quencher acceptor in Fig. 4D (Lee et al., 2018). This method holds remarkable merits in extensive applications for the measurement of MMP enzyme family and rapid evaluation of anticancer compounds. And Qian described a switchable FRET system based on telomerase-responsive MSN to realize in situ "off-on" imaging of intracellular telomerase activity (Fig. 5A) (Qian et al., 2013). After loading fluorescein into the mesopores, MSN was wrapped by DNA (O1) to obtain a telomerase-responsive biosensor. In the presence of telomerase, the biosensor could generate fluorescence because of the detachment of O1 on the surface of the MSN.

Several researches have also fabricated FRET biosensors for the detection of proteases collagenase (MMP-9, MMP-2), thioredoxin

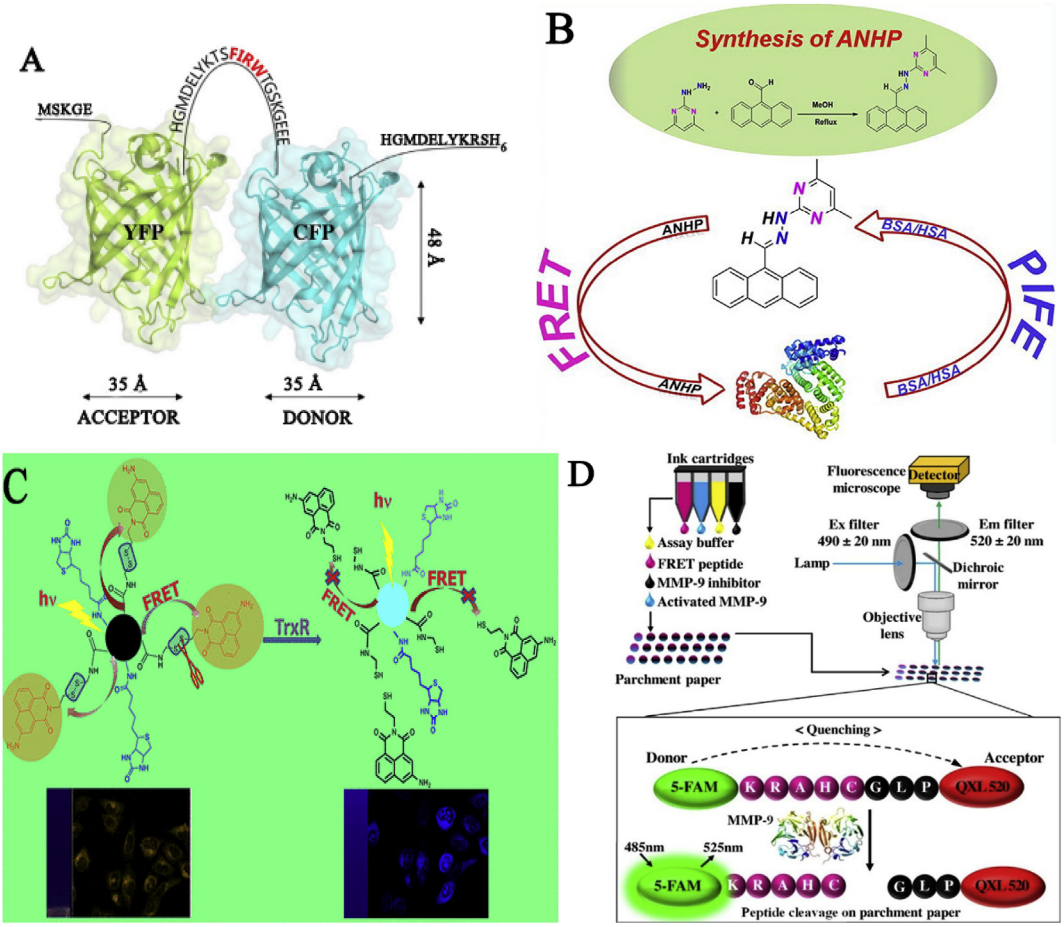

Fig. 4. (A) Schematic illustration of FRET-based biosensors based on a fluorophore protein pairs for the detection of NE activity. Reprinted (adapted) with permission from Faccio and Salentinig (2017). (B) FRET-based biosensor for the detection of protein conformational change. Reprinted (adapted) with permission from Ghosh et al. (2018). (C) A highly selectively FRET biosensor for monitoring of the activity of TrxR. Reprinted (adapted) with permission from Sidhu et al. (2017). (D) Diagram of biosensor based on a quencher and fluorophore for the target of MMP-9 in anticancer screening assay. Reprinted (adapted) with permission from Lee et al. (2018).

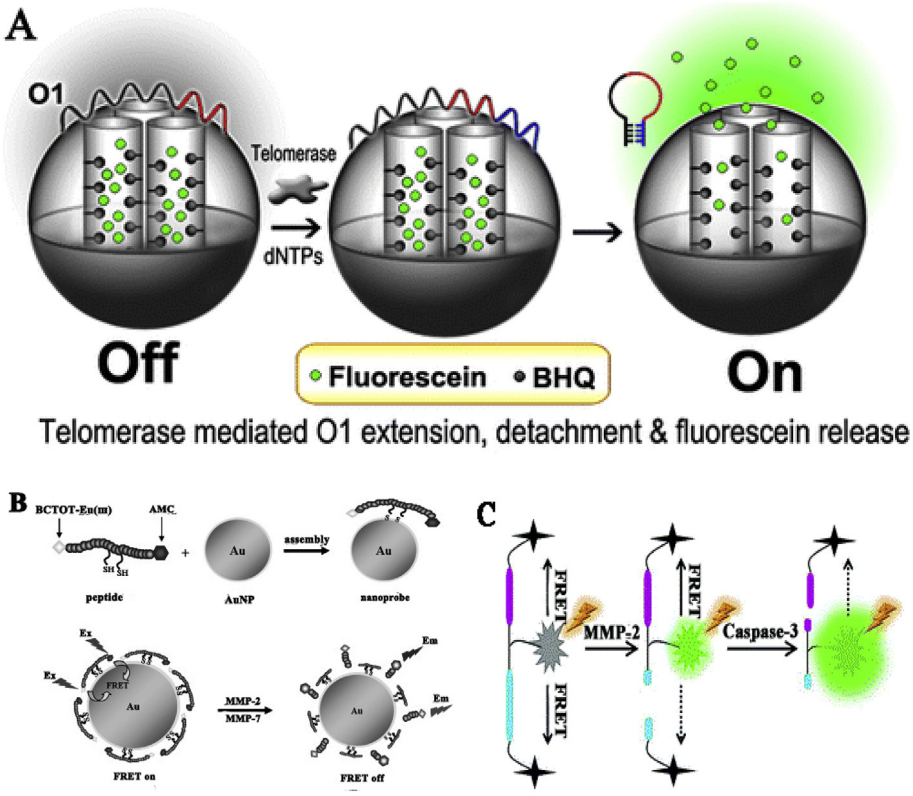

Fig. 5. (A) Schematic illustration of FRET nanocarrier based on MSN for living cell imaging. Reprinted (adapted) with permission from Qian et al. (2013). (B) A dual-FRET biosensor for detecting MMP-2 and MMP-7. Reprinted (adapted) with permission from Wang et al. (2012). (C) Structure of dual-FRET biosensor for two targeted analytes, MMP-2 and caspase-3. Reprinted (adapted) with permission from Li et al. (2015).

reductase, caspase-3 and others zymoproteins in living cells (Shi et al., 2006; Ren et al., 2014; Kwon et al., 2017). These enzymes in pathological state are over-expressed, in which case the biosensors in the surrounding medium may respond adequately. Xu designed a dual-labeled FRET-based biosensor for the simultaneous imaging of MMP-2 and MMP-7 of living cells under single wavelength excitation as shown in Fig. 5B (Wang et al., 2012). MMP-sensitive biosensor was prepared by bio-conjugating a double-labeled fluorescent cleavable peptide spacer, where 7-amino-4-methylcoumarin (AMC) and 1,10-bis(5′-chlorosulfothiophene-2′-yl) −4,4,5,5,6,6,7,7-octafluorodecane-1,3,8,10 -etraone (BCTOT-Eu^{III}) was respectively combined to the N terminus and the C terminus of two substrate peptides (a MMP-2 substrate and a MMP-7 substrate), onto the surface of Au NPs through cysteine residues of peptide substrate. At the presence of the complexes of MMP-2 and MMP-7, the FRET process of biosensor was destructed, and the fluorescence of dye was recovered at 449 nm and 613 nm. The strategy exhibits high specificity against BSA and normal-cell for simultaneous imaging of dual components of MMP-2 and MMP-7 in a complex system, and the biosensor can effectively avoid negative outcomes in cancer cell diagnosis (Wang et al., 2012). Li also designed a dual-FRET biosensor to target MMP-2 and caspase-3 for screening of cancer drug and therapeutic effect evaluation as shown in Fig. 5C (Li et al., 2015). The FRET system is comprised of quencher-fluorophore pairs, a 5 (6)-carboxyfluorescein (FAM) (donor) and two Dabcyl molecules (accepter), and the cleavable substrates containing MMP-2 specific peptide unit and caspase-3 sensitive peptide sequence.

And the improvement of monitoring the enzymatic activity at the surface of living cells using a FRET-based biosensor was also achieved by Limsakul (Limsakul et al., 2018). They reported a hybrid biosensor for in situ monitoring the mombrane type 1 matrix metalloproteinase (MT1 MMP) activity. The successfully integrating of monobody variant (PEbody, a specific binding partner for R-phycoerythrin (R-PE)) into a FRET biosensor was capable to monitor cell-cell junction maturity for the dynamic formation and dissociation of cell-cell contacts.

3.4. Nucleic acid-based FRET biosensor

DNA or RNA molecules, such as aptamers, could specifically combine with the complementary targets by typical Watson-Crick based-pairing, or bind with the targets including small molecules, proteins and larger cells by specific folding three-dimensional conformations (Famulok et al., 2007; Ma et al., 2015). Specific combination exhibited huge merits such as high affinity, selectivity, stability, low cost and high thermal stability as shown in Table 3 (Chen et al., 2014; Yuan et al., 2014). Most hybridization assays of nucleic acid-sensing FRET biosensors were achieved by the sandwich, displacement and non-specific assemblies (Auer et al., 2017; Tian et al., 2017; Wu et al., 2018; Climent et al., 2010).

Alexander Auer reported a fast, background-free FRET biosensor for DNA point accumulation in nanoscale topography (DNA-PAINT) imaging by the predictable and transient hybridization between short “imager” labeled by dyes and complementary target-bound “docking” strands (Fig. 6A) (Auer et al., 2017). This biosensor could achieve high-quality and super-resolution imaging of DNA for dynamic process in cellular environment in few tens of seconds. Jepsen developed a FRET biosensor, in which using fluorescent RNA aptamers to produce a dynamic and reversible RNA nanodevice for tracking RNA molecules in *E. coli* (Jepsen et al., 2018).

A FRET ratiometric aptasensor was designed for the detection of ochratoxin A (OTA) in feed and food chains by using colloidal cerium oxide nanoparticles (the donor) and graphene quantum dots (GQDs, the acceptor) (Tian et al., 2017). In this biosensor, DNA@nanoceria and DNA@GQD was designed to complement with OTA aptamer by the electrostatic force as shown in Fig. 6B. The aptasensor exhibited a satisfying linear range (0.01–20 ng mL^{-1}), a low limit of detection (2.5 pg mL^{-1}), and high selectivity towards OTA. Wu et al. designed a highly efficient FRET biosensor for DNA hybridization detection by using small upconversion nanoparticles (UCNPs) and nucleic acid stain SYBR Green I (SG, a specific intercalator of double-stranded DNA) as shown in Fig. 6C (Wu et al., 2018). The 10-nm-UCNP-based DNA

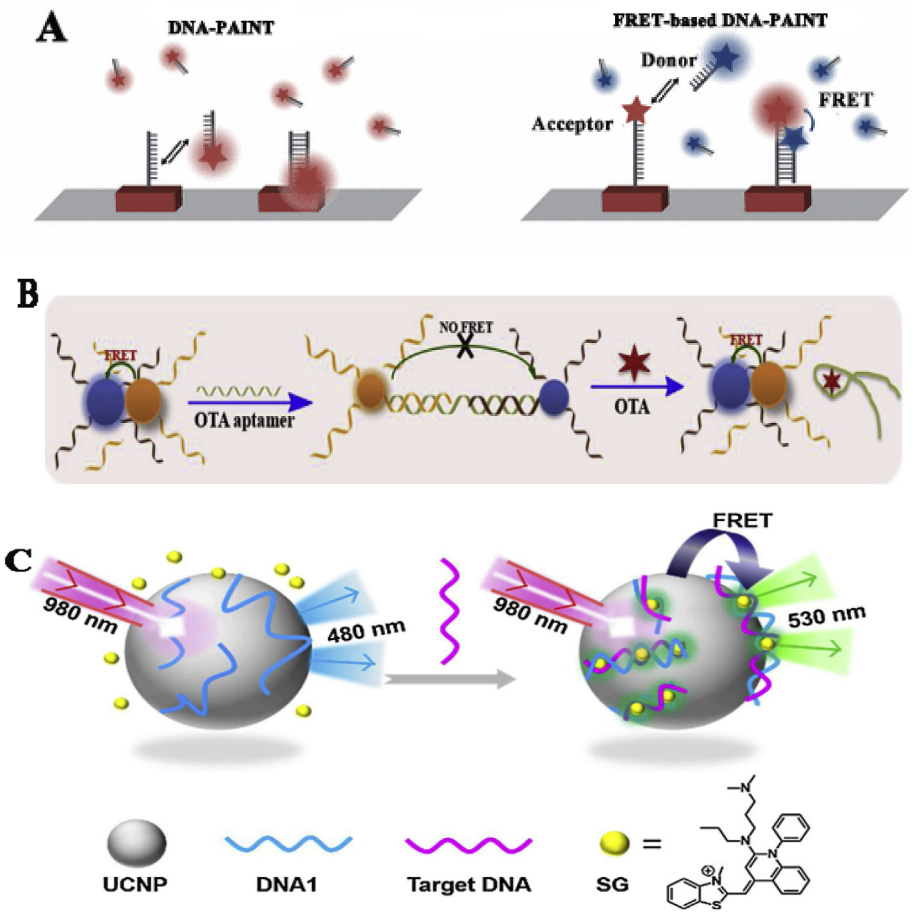

Fig. 6. (A) Comparison diagram of FRET-based and conventional probe for DNA-PAINT imaging by hybridization. Reprinted (adapted) with permission from Auer et al. (2017). (B) A ratiometric aptasensor for the detection of OTA in feed and food. Reprinted (adapted) with permission from Tian et al. (2017). (C) Schematics of near-infrared responsive FRET-based DNA biosensor based on UCNPs and SG for exploring the optimal nanoparticle size. Reprinted (adapted) with permission from Wu et al. (2018).

biosensor could reach a lower detection limit of complementary ssDNA at 3.2 nM and three-base mismatched ssDNA2-M3 at 7.6 nM. Xu also demonstrated a FRET biosensor based on miRNA-directed intracellular self-assembly of chiral nanorod dimers (Xu et al., 2018).

3.5. Tissue-based biosensor

FRET has also been successfully used for tissue-based biosensor (Bouchaala et al., 2016; Mei et al., 2007; Campas et al., 2008; Guo and Tan, 2010; Chen et al., 2011; Guo et al., 2018). Bouchala fabricated a fluorescent nano-emulsion droplets (NDs) of 100 nm size by encapsulating lipophilic near-infrared cyanine 5.5 and 7.5 dye into nano-emulsion droplets with the help of hydrophilic counterion tetraphenylborate for *vivo* imaging as shown in Fig. 7 (Bouchaala et al., 2016). This biosensor indicated that the integrity of the FRET NCs in the blood circulation of healthy mice is preserved at 93% at 6 h of post-administration, while it drops to 66% in the liver (half-life is 8.2 h). Chen et al. fabricated an acid-active tumor targeting nanoplatform 2,3-dimethylmaleic anhydride (DA)-trans-activating transcriptional activator (TAT)- poly (ε-caprolactone) (PEG-PCL, PECL) to inhibit the nonspecific interactions of TAT in the bloodstream. The FRET signal between camptothecin (CPT) and maleimide thioether bond is monitored to visualize the drug release process (Guo et al., 2018).

3.6. Other FRET sensors

Although the distance from the donor to the accepter is the main effect in the FRET system, a multi-FRET biosensor with independent distance was also reported. Saha reported a multi-step FRET system for the study of molecular level by using three dyes, pyrene (Py), Acriflavine (Acf) and Rhodamine B (RhB) as shown in Fig. 8A (Saha et al., 2016). As an energy transfer platform, Acf could receive energy from Py and then transfer energy to RhB. This multi-step FRET process has advantageous merits for the studying molecular level interaction beyond conventional FRET distance (1–10 nm) and multi-branched macromolecules. And the incorporation of nanoclay laponite could enhance the transfer efficiency of FRET.

Moreover, a molecularly imprinted fluorescent biosensor based on FRET was developed for the detection of doxorubicin. This system was utilized doxorubicin as the template to fabricate a molecularly imprinted polymer thin layer onto the surface of modified silica nanosphere modified by CD through sol-gel polymerization. The FRET biosensor showed high sensitivity and selectivity for doxorubicin with the detection limit of 13.8 nM (Xu et al., 2017).

FRET has also been used for thermal biosensor (Kearney et al., 2013; Conde et al., 2016; Kim et al., 2012; Zhou et al., 2015), where biosensors were assimilated into a physical transducer. Huang fabricated a FRET nano-platform for monitoring thermos-sensitive nanoscale assembly of polymeric micelles into hydrogel and release process of micelles (Huang et al., 2017). The thermo-sensitive "micellar hydrogel" was prepared based on poly (ε-caprolactone-*co*-1,4,8-trioxa [4.6] spiro-9-undecanone)-b-poly (ethyleneglycol)-*b*-poly (ε-caprolactone-o-1,4,8-trioxa [4.6]spiro-9-undecanone) (PECT) triblock copolymer in Fig. 8C. In this system, FITC as a donor and rhodamine B (RB) as an acceptor were separately conjugated to PECT polymers to obtain the PECT-FITC and PECT-RB nanoparticle. The micelles co-assembled by PECT-FITC and PECT-RB polymers within the range of 10 nm will generate strong emission at 590 nm at excitation of 465 nm. This hydrogel was injected into rat to tract the local delivery and degradation of micelles through FRET imaging. The thermos-sensitive biosensor facilitates the hydrogel formation and the sustained shedding of cognate micelles (Huang et al., 2017). By using the multiple-tags based FRET-imaging technology, the

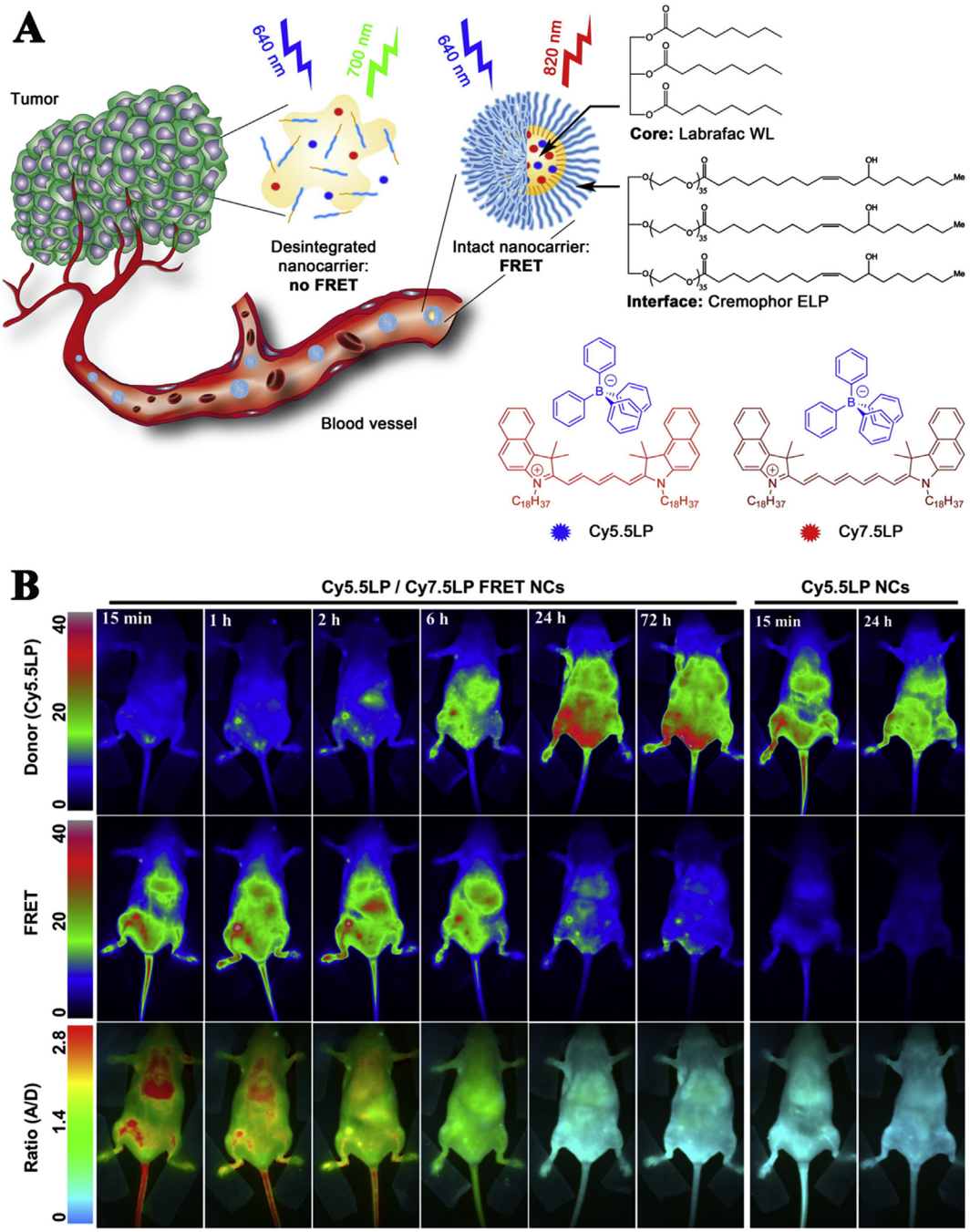

Fig. 7. Integrity of lipid nanocarriers in bloodstream and tumor quantified by near-infrared ratiometric FRET imaging in living mice. Reprinted (adapted) with permission from Bouchaala et al. (2016).

fate of macro biodegradable materials *in vitro* and *in vivo* can be followed at a precise nano even molecular level.

4. Conclusions

FRET-based biosensors have been exploited for quantitative analysis of small molecular *in vitro*, real-time monitoring the dynamics of the compound in/on the surface of living cells and *in vivo* for biological applications. And their applications have also been extended to the medical diagnostics. Nanomaterial-based biosensors possess great attractive prospects in clinical diagnosis, food analysis, process and environmental monitoring. The successful immobilization of the fluorophore into nanomaterial could present an advantage of stability in the FRET system. FRET biosensors, as the advantageous non-invasive procedure, are valuable imaging methods for visualization of specific molecular activity during significant cellular process. The development of novel FRET system, such as multi-FRET system, and the specific receptor for the analysis would be beneficial for the fabrication of biosensors. The applications of FRET-based biosensors for cellular processes, disease diagnostics, and medical drug therapy, will undoubtedly be of great significance.

Future perspectives

Extensive researches have been demonstrated that FRET-based biosensors are promising and non-invasive tools for monitoring the

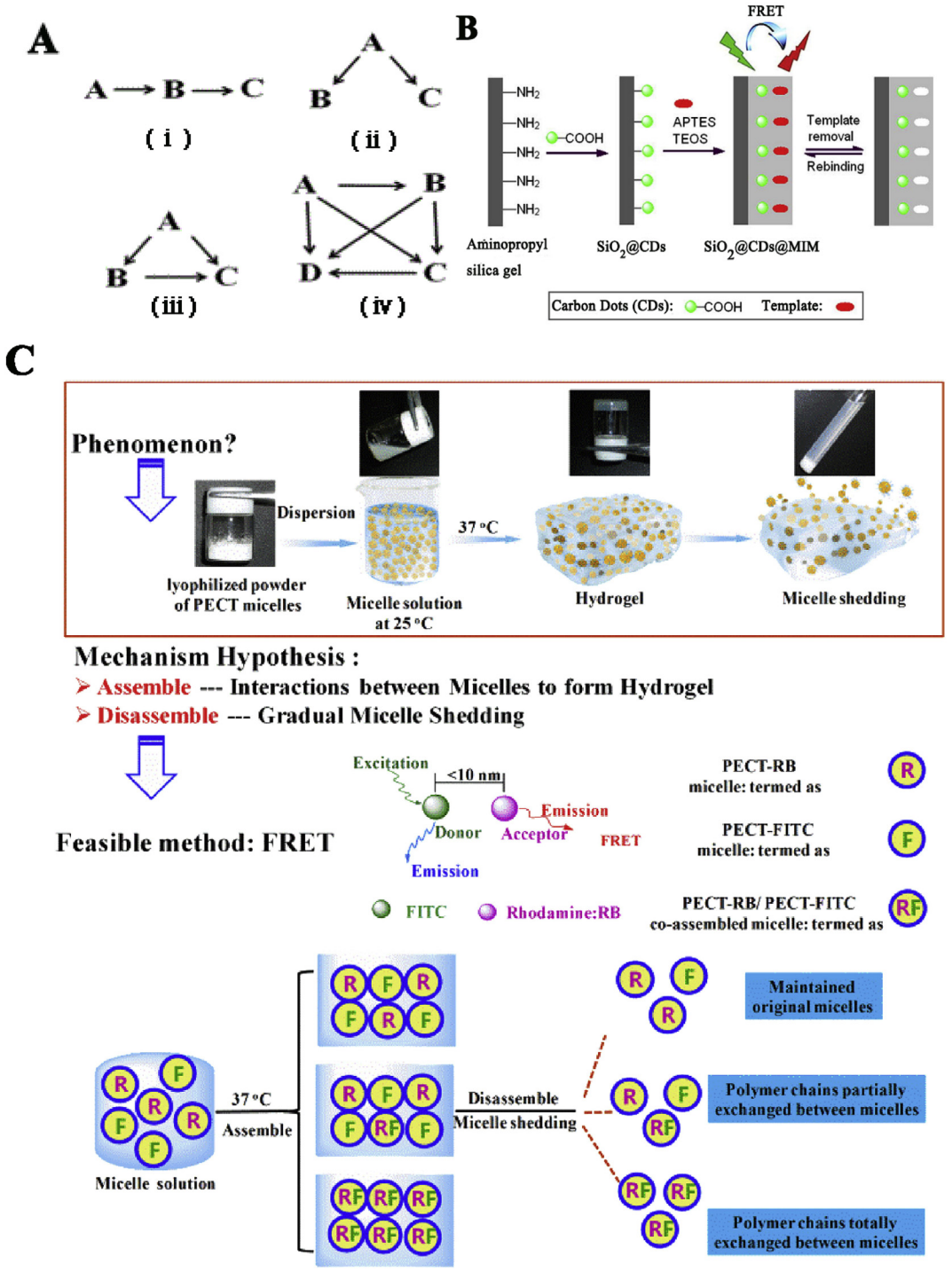

Fig. 8. (A) Multi-step FRET biosensor for studying molecular level interaction from Pyrene (Py) to Rhodamine B (RhB) via Acriflavine (Acf). Reprinted (adapted) with permission from Saha et al. (2016). (B) Molecularly imprinted FRET biosensor for selective and sensitive detection of doxorubicin. Reprinted (adapted) with permission from Xu et al. (2017). (C) FRET biosensor for the monitoring of the thermosensitive nanoscale assembly of polymeric micelles into macroscale hydrogel and sequential cognate micelles release. Reprinted (adapted) with permission from Huang et al. (2017).

dynamic change of the small-molecular, proteins and living cell in laboratory environments. Despite of the various applications, FRET-based biosensors have many significant challenges in high-fluorescent resolution, improved specificity of the reaction, and the affordability of FRET reagents. For example, the strategy for enhancing the ratio of signal/noise is major challenge. Governing the surface property of the nanoscale composites by a novel functional group is also great challenge for the presently existing techniques. Moreover, dynamic monitoring for physiological conditions in real time reversibly is also major impediments. Future work should focus on the fabrication of new FRET system such as multi-FRET biosensor. And more fluorophores in multi-step FRET system should be chosen for the detection of some larger molecular. Besides, the development of FRET has appeared many of variation, including bioluminescence and chemiluminescence resonance energy transfer, and which would be beneficial for the biological research.

Acknowledgements

We sincerely appreciate the National Natural Science Foundation of China for the financial support (81573388). This work was supported by “Qing Lan Project of Jiangsu province” and “Six talent peaks project of Jiangsu Province (YY-032)”. This work was also supported by the Open Project Program of Jiangsu Key Laboratory for Pharmacology and Safety Evaluation of Chinese Materia Medica (No. JKLPSE201805) and the Project of the Priority Academic Program Development of Jiangsu Higher Education Institutions (PAPD).

References

Albers, A.E., Okreglak, V.S., Chang, C.J., 2006. J. Am. Chem. Soc. 128, 9640–9641.
Albert, K.J., Walt, D.R., 2000. Anal. Chem. 72, 1947–1955.
Auer, A., Strauss, M.T., Schlichthaerle, T., Jungmann, R., 2017. Nano Lett. 17, 6428–6434.
Balzani, V., Ceroni, P., Gestermann, S., Gorka, M., Kaufmann, C., 2000. J. Chem. Soc. 246, 3765–3771.
Barker, S.L., Kopelman, R., Meyer, T.E., Cusanovich, M.A., 1998. Anal. Chem. 70, 971–976.
Berney, C., Danuser, G., 2003. Biophys. J. 84, 3992–4010.
Bouchaala, R., Mercier, L., Andreiuk, B., Mély, Y., Vandamme, T., 2016. J. Control. Release 236, 57–67.
Bremer, C., Tung, C.H., Weissleder, R., 2001. Nat. Med. 7, 743–748.
Campas, M., Carpentier, R., Rouillon, R., 2008. Biotechnol. Adv. 26, 370–378.
Cao, L., Wang, X., Meziani, M.J., Lu, F., Wang, H., Luo, P.G., Lin, Y., Harruff, B.A., Veca, L.M., Murray, D., Xie, S.Y., Sun, Y.P., 2007. J. Am. Chem. Soc. 129, 11318–11319.
Charron, D.M., Chen, J., Zheng, G., 2015. Cancer Treat Res. 166, 103–127.
Charron, D.M., Zheng, G., 2018. Nano Today 18, 124–136.
Chen, G., Roy, I., Yang, C., Prasad, P.N., 2016. Chem. Rev. 116, 2826–2885.
Chen, H., Puhl, H.L., Ikeda, S.R., 2007. J. Biomed. Opt. 12, 054011.
Chen, H., Zhang, W., Zhu, G., Xie, J., Chen, X., 2017. Nat. Rev. Mater 2, 17024.
Chen, L., Wu, Y., Lin, Y., Wang, Q., 2015. Chem. Commun. 51, 10190–10193.
Chen, Q., Xiao, L.D., Liu, Q.J., Ling, S.C., Yin, Y.F., Dong, Q., Wang, P., 2011. Biosens. Bioelectron. 26, 3313–3319.
Chen, X., Huang, Y., Duan, N., Wu, S., Xia, Y., 2014. Microchim, Microchimica Acta 181, 1317–1324.
Clapp, A.R., Medintz, I.L., Mauro, J.M., Fisher, B.R., Bawendi, M.G., Mattoussi, H., 2004. J. Am. Chem. Soc. 126, 301–310.
Climent, E., Martínez-Máñez, R., Sancenón, F., Marcos, M.D., Soto, J., 2010. Angew. Chem. Int. Ed. 49, 7281–7283.
Conde, J., Oliva, N., Atilano, M., Song, H.S., Artzi, N., 2016. Nat. Mater. 15, 353–363.
Corry, B., Jayatilaka, D., Rigby, P., 2005. Biophys. J. 89, 3822–3836.
Culotta, E., Koshland, D.E., 1992. Science 258, 1862–1865.
Du, J.J., Gu, Q.Y., Chen, J.Y., Fan, J.L., Peng, X.J., 2018. Sensor. Actuator. B Chem. 265, 204–210.
Duncan, K.E., Ngu, T.T., Chan, J., Salgado, M.T., Merrifield, M.E., 2006. Exp. Biol. Med. 231, 1488–1499.
Ekdawi, S.N., Stewart, J.M., Dunne, M., tapleton, S., Mitsakakis, N., 2015. J. Control. Release 207, 101–111.
Enterina, J.R., Wu, L.S., Campbell, R.E., 2015. Curr. Opin. Chem. Biol. 27, 10–17.
Faccio, G., Salentinig, S., 2017. Biophys. J. 113, 1731–1737.
Famulok, M., Hartig, J.S., Mayer, G., 2007. Chem. Rev. 38, 3715–3743.
Feng, L., Bi, P.Q., Yang, X.Y., Niu, M.S., Zhang, K.N., Wang, F., Lv, C.K., Wen, Z.C., Hao, X.T., 2018. Org. Electron. 57, 140–145.
Fommer, W.B., Davidson, M.W., Campbell, R.E., 2009. ChemInform 40, 2833–2841.
Gadella, T.W., 2009. ElsevierScience Amsterdam 33.
Ghosh, S., Singharoy, D., Bhattacharya, S.C., 2018. Biomolecular Spectroscopy 195, 7–15.
Goldsmith, S.J., 1975. Semin. Nucl. Med. 5, 125–152.
Guo, X., Wang, L., Duval, K., Fan, J., Zhou, S.B., Chen, Z., 2018. Adv. Mater. 30, 1705436.
Guo, Y., Tan, J.L., 2010. Biosens. Bioelectron. 25, 1958–1962.
Guo, Z., Park, S., Yoon, J., Shin, I., 2013. Chem. Soc. Rev. 43, 16–29.
Haab, B.B., 2003. Proteomics 3, 2116–2122.
He, L., Wu, X., Meylan, F., Olson, D.P., Simone, J., 2004. Am. J. Pathol. 164, 1901–1913.
Hildebrandt, N., Spillmann, C.M., Algar, W.R., Pons, T., Stewart, M.H., 2017. Chem. Rev. 117, 536–711.
Horvath, G., Petras, M., Szentesi, G., Fabian, A., Park, J.W., Vereb, G., Szollosi, J., 2005. Cytometry 65, 148–157.
Hu, B., Hu, L.L., Chen, M.L., Wang, J.H., 2013. Biosens. Bioelectron. 49, 499–505.
Hu, F., Zheng, B., Wang, D., Liu, M., Du, J., 2014. Analyst 139, 3607–3613.
Huang, P., Song, H., Zhang, Y., Liu, J., Cheng, Z., 2017. Biomaterials 145, 81–91.
Ibraheem, A., Campbell, R.E., 2010. Curr. Opin. Chem. Biol. 14, 30–36.
James, M.L., Gambhir, S.S., 2012. Physiol. Rev. 92, 897–965.
Jepsen, M.D.E., Sparvath, S.M., Nielsen, T.B., 2018. Nat. Commun. 9.
Jin, T., Sasaki, A., Kinjo, M., Miyazaki, J., 2010. Chem. Commun. 46, 2408–2410.
Jin, Z.W., Geißler, D., Qiu, X., Wegner, K.D., Hildebrandt, N., 2015. Angew. Chem. Int. Ed. 4, 10024–10029.
Kaafarani, B.R., Wex, B., Wang, F., Catanescu, O., Chien, L.C., Neckers, D.C., 2003. J. Org. Chem. 68, 5377–5380.
Kattke, M.D., Gao, E.J., Sapsford, K.E., Stephenson, L.D., Kumar, A., 2011. Sensors 11, 6396–6410.
Kearney, C.J., Mooney, D.J., 2013. Nat. Mater. 12, 1004–1017.
Kikhney, A.G., Svergun, D.I., 2015. FEBS Lett. 589, 2570–2577.
Kikuchi, K., Takakusa, H., Nagano, T., 2004. Trac. Trends Anal. Chem. 23, 407–415.
Kim, Y.M., Park, M.R., Song, S.C., 2012. ACS Nano 6, 5757–5766.
Klymchenko, A.S., 2017. Acc. Chem. Res. 50, 366.
Knopp, D., 2006. Anal. Bioanal. Chem. 385, 425–427.
Kobayashi, H., Ogawa, M., Alford, R., Choyke, P.L., Urano, Y., 2010. Chem. Rev. 110, 2620–2640.
Kumar, M., Guo, Y.P., Zhang, P., 2009. Biosens. Bioelectron. 24, 1522–1526.
Kunjachan, S., Ehling, J., Storm, G., Kiessling, F., Lammers, T., 2015. Chem. Rev. 115, 10907–10937.
Kwon, E.J., Dudani, J.S., Bhatia, S.N., 2017. Nat Biomed Eng 1, 0054.
Kyrychenko, A., Rodnin, M.V., Ghatak, C., Ladokhin, A.S., 2017. Data in Brief 12, 213–221.
Lai, J., Shah, B.P., Garfunkel, E., Lee, K.B., 2013. ACS Nano 7, 2741–2750.
Lakowicz, J.R., Masters, B.R., 1991. Naturwissenschaften 78, 456–457.
Lane, L.A., Qian, X., Smith, A.M., Nie, S., 2015. P Annual Review of Physical Chemistry 66, 521.
Lee, J., Samson, A.A., Song, J.M., 2018. Sensor. Actuator. B Chem. 256, 1093–1099.
Leeuwen, F.W., Hardwick, J.C., Erkel, A.R., 2015. Radiology 276, 12–29.
Lequin, R.M., 2005. Clin. Chem. 51, 2415–2418.
Li, L., Guan, R., Guo, M., Ning, P., Shao, R., 2017. Sensor. Actuator. B Chem. 254, 949–955.
Li, L.L., Wu, G.H., Yang, G.H., Peng, J., Zhao, J.W., Zhu, J.J., 2013. Nanoscale 5, 4015–4039.
Li, S.Y., Liu, L.H., Cheng, H., Li, B., Qiu, W.X., 2015. Chem. Commun. 51, 14520–14523.
Liao, J.Y., Song, Y., Liu, Y., 2015. Acta Pharmacol. Sin. 36, 1408–1415.
Limsakul, P., Peng, Q., Wu, Y.Q., Allen, M.E., Liang, J., Remacle, A.G., Lopez, T., Ge, X., Kay, B.K., Zhao, H., Strongin, A.Y., Yang, X.L., Lu, S.Y., 2018. Cell Chemical Biology 25, 1–10.
Liu, Y., Wang, Y.M., Zhu, W.Y., Zhang, C.H., Tang, H., Jiang, J.H., 2018. Anal. Chim. Acta 1012, 60–65.
Lu, H.Z., Quan, S., Xu, S.F., 2017. J. Agric. Food Chem. 65, 9807–9814.
Luby, B.M., Charron, D.M., Maclaughlin, C.M., Zheng, G., 2016. Adv. Drug Deliv. Rev. 113, 97–121.
Luo, S., Zhang, E., Su, Y., Cheng, T., Shi, C., 2011. Biomaterials 32, 7127–7138.
Ma, H., Liu, J., Ali, M.M., Mahmood, M.A.I., Labanieh, L., Lu, M., Iqbal, S.M., Zhang, Q., Zhao, W., Wan, Y., 2015. Chem. Soc. Rev. 44, 1240–1256.
Maxwell, D.J., Taylor, J.R., Nie, S.M., 2002. J. Am. Chem. Soc. 124, 9606–9612.
Mccartney, C.E., Macleod, J.A., Greer, P.A., Davies, P.L., 2017. Biochim. Biophys. Acta 1865, 221–230.
Medintz, I.L., Clapp, A.R., Mattoussi, H., Goldman, E.R., Fisher, B.J., 2003. Nat. Mater. 2, 630–638.
Mehrotra, P., 2016. J. Oral Biol Craniofac Res. 6, 153–159.
Mei, Y., Ran, L., Ying, X., Yuan, Z., Xin, S., 2007. Biosens. Bioelectron. 22, 871–876.
Mertens, H.D., Piljić, A., Schultz, C., Svergun, D.I., 2012. Biophys. J. 102, 2866–2875.
Mirkin, C.A., Meade, T.J., Petrosko, S.H., Stegh, A.H., 2015. 166. Springer International Publishing, pp. 481–501.
Mohsin, M., Ahmad, A., 2014. Biosens. Bioelectron. 59, 358–364.
Mohsin, M., Diwan, H., Khan, I., Ahmad, A., 2015. Biochem. Eng. J. 102, 62–68.
Morris, M.C., 2010. Cell Biochem. Biophys. 56, 19–37.
Mura, S., Couvreur, P., 2012. Adv. Drug Deliv. Rev. 64, 1394–1416.
Pansare, V., Hejazi, S., Faenza, W., Prud, R.K., 2012. Chem. Mater. 24, 812–827.
Park, J.H., Maltzahn, G., Zhang, L., Derfus, A.M., Simberg, D., Harris, T.J., Ruoslahti, E., Bhatia, S.N., Sailor, M.J., 2009. Small 5, 694–700.
Pelaz, B., Alexiou, C., Alvarez-Puebla, R.A., Alves, F., Andrews, A.M., 2017. Acs Nan 11, 2313–2381.
Periasamy, A., 2001. J. Biomed. Opt. 6, 287–291.
Peroza, E.A., Ewald, J.C., Parakkal, G., Skotheim, J.M., Zamboni, N., 2015. Anal. Biochem. 474, 1–7.
Petersen, A.L., Hansen, A.E., Gabizon, A., Andresen, T.L., 2012. Adv. Drug Deliv. Rev. 64, 1417–1435.
Priem, B., Tian, C., Tang, J., Zhao, Y., Mulder, W.J., 2015. Expert Opin. Drug Deliv. 12, 1881–1894.
Pulli, T., Hoyhtya, M., Soderlund, H., Takkinen, K., 2002. Anal. Chem. 77, 2637.
Qian, R., Ding, L., Ju, H., 2013. J. Am. Chem. Soc. 135, 13282–13285.
Qin, Q.P., Peltola, O., Pettersson, K., 2003. Clin. Chem. 49, 1105.
Rai, M., Jogee, P.S., Ingle, A.P., 2015. Int. J. Food Sci. Nutr. 66, 363–370.
Raicu, V., 2007. J. Biol. Phys. 33, 109–127.
Ray, P.C., Fan, Z., Crouch, R.A., Sinha, S.S., Pramanik, A., 2014. Chem. Soc. Rev. 43, 6370–6404.
Rehm, M., Dussmann, H., Janicke, R.U., Tavare, J.M., Kogel, D., 2002. J. Biol. Chem. 277, 24506–24514.
Ren, D.H., Wang, J., You, Z., 2014. RSC Adv. 4, 54907–54918.
Russ Algar, W., Susumu, K., bDelehanty, J.B., Medintz, I.J., 2011. Anal. Chem. 83, 8826–8837.
Saha, J., Dey, D., Roy, A.D., Bhattacharjee, D., Hussain, S.A., 2016. J. Lumin. 172, 168–174.
Saha, J., Roy, A.D., Dey, D., Bhattacharjee, D., Hussain, S.A., 2018. Mater. Today: Proceedings 5, 2306–2313.
Samanta, S., Halder, S., Dey, P., Manna, U., Rameshand, A., Das, G., 2018. Analyst 143 250-25.
Sapsford, K.E., Berti, L., Medintz, I.L., 2006. Angew. Chem. Int. Ed. 45, 4562–4589.
Selvin, P.R., 2005. Annu. Rev. Biophys. Biomol. Struct. 31, 275–302.
Shen, J., Li, Y., Gu, H., Xia, F., Zuo, X., 2014. Chem. Rev. 114, 7631–7677.
Shi, L., De Paoli, V., Rosenzweig, N., Rosenzweig, Z., 2006. J. Am. Chem. Soc. 128,

10378–10379.
Sidhu, J.S., Singh, A., Garg, N., Singh, N., 2017. ACS Appl. Mater. Interfaces 9, 25847–25856.
Smith, B.R., Gambhir, S.S., 2017. Chem. Rev. 117, 901–986.
Song, K., Kong, X., Liu, X., Zhang, Y., Zeng, Q., Tu, L., 2012. Chem. Commun. 48, 1156–1158.
Strianese, M., De, M.F., Pavone, V., Lombardi, A., Canters, G.W., 2010. J. Inorg. Biochem. 104, 619–624.
Stringer, R.C., Hoehn, D., Grant, S.A., 2008. IEEE Sens. J. 8, 295–300.
Sun, M.T., Du, L.B., Yu, H., Zhang, K., Liu, Y., Wang, S.H., 2017. Talanta 162, 180–186.
Sun, Y., Wallrabe, H., Seo, S.A., Periasamy, A., 2010. ChemPhysChem 12, 462–474.
Thapaliya, E.R., Fowley, C., Callan, B., Tang, S., Zhang, Y., 2015. Langmuir the Acs Journal of Surfaces & Colloids 31, 9557–9565.
Thévenot, D.R., Toth, K., Durst, R.A., Wilson, G.S., 2001. Biosens. Bioelectron. 34, 635–659.
Thevenot, D.R., Toth, K., Durst, R.A., Wilson, G.S., 1999. Pure Appl. Chem. 71, 2333–2348.
Tian, A.J., Wei, W., Wang, J., Ji, S., Chen, G., 2017. Anal. Chim. Acta 1000, 265–272.
Tian, Y.Q., Su, F.Y., Weber, W., Nandakumar, V., Shumway, B.R., Jin, Y.G., Zhou, X.F., Holl, M.R., Johnson, R.H., Meldrum, D.R., 2010. Biomaterials 31, 7411–7422.
Torchilin, V.P., 2005. Nat. Rev. Drug Discov. 4, 145–160.
Torchilin, V.P., 2014. Nat. Rev. Drug Discov. 13, 813–827.
Toy, R., Bauer, L., Hoimes, C., Ghaghada, K.B., Karathanasis, E., 2014. Adv. Drug Deliv. Rev. 76, 79–97.
Vicinelli, V., Ceroni, P., Maestri, M., Balzani, V., Gorka, M., 2002. J. Am. Chem. Soc. 124, 6461–6468.
Wang, P., Joshi, P., Alazemi, A., Zhang, P., 2014. Biosens. Bioelectron. 62, 120–126.
Wang, X., Niessner, R., Tang, D., Knopp, D., 2016. Anal. Chim. Acta 912, 10–23.
Wang, X., Xia, Y.Q., Liu, Y.Y., Qi, W.X., Sun, Q.Q., Zhao, Q., Tang, B., 2012. Chemistry 18, 7189–7195.
Wang, X., Yu, S., Liu, W., Fu, L., Wang, Y., Li, J., Chen, L., 2018. ACS Sens. 3, 378–385.
Webster, T.J., 2006. Int. J. Nanomed. 1, 115–116.
Wu, B., Cao, Z., Zhang, Q., Wang, G., 2018. Sensor. Actuator. B 255, 2853–2860.
Xu, L.G., Gao, Y.F., Kuang, H., Liz-Marzán, L.M., Xu, C.L., 2018. Angew Chem. Int. Ed. Engl. 57, 10544–10548.
Xu, W., Xiong, Y., Lai, W., Xu, Y., Li, C., 2014. Biosens. Bioelectron. 56, 144–150.
Xu, Z.F., Deng, P.H., Li, J.H., Xu, L., Tang, S.P., 2017. Mater. Sci. Eng., B 218, 31–39.
Yan, X., Li, B.S., Li, L.S., 2013. Acc. Chem. Res. 46, 2254–2262.
Yao, J., Yang, M., Duan, Y., 2014. Chem. Rev. 114, 6130–6178.
Yuan, F., Chen, H., Xu, J., Zhang, Y., Wu, Y., 2014. Chemistry 20, 2888–2894.
Yuan, L., Jin, F., Zeng, Z., Liu, C., Luo, S., 2015. Chem. Sci. 6, 2360.
Yuan, L., Lin, W., Zheng, K., Zhu, S., 2013. Acc. Chem. Res. 46, 1462–1473.
Yue, D.F., Wang, M.L., Deng, F., Yin, W.T., Zhao, H.D., Zhao, X.M., Xu, Z.C., 2018. Chin. Chem. Lett. 29, 648–656.
Zadran, S., Standley, S., Wong, K., Otiniano, E., Amighi, A., 2012. Appl. Microbiol. Biotechnol. 96, 895–902.
Zahavy, E., Fisher, M., Bromberg, A., Olshevsky, U., 2003. Appl. Environ. Microbiol. 69, 2330–2339.
Zhang, C., Yuan, Y., Zhang, S., Wang, Y., Liu, Z., 2011. Angew. Chem. Int. Ed. 50, 6851–6854.
Zhang, P., Rogelj, S., Nguyen, K., Wheeler, D., 2006. J. Am. Chem. Soc. 128, 12410–12411.
Zhang, X.J., Miao, Z.Y., Hu, Y., Yang, X.T., Tang, Y.Y., Zhu, D., 2018. Sensor. Actuator. B Chem. 273, 511–518.
Zhang, X.L., Xiao, Y., Qian, X.H., 2008. Angew. Chem. Int. Ed. 47, 8025–8029.
Zhao, W.Q., Liu, X.L., Lv, H.T., Fu, H., Yang, Y., Huang, Z.P., Han, A., 2015. Tetrahedron Lett. 56, 4293–4298.
Zheng, F.F., Zhang, P.H., Xi, Y., Chen, J.J., Li, L.L., 2015. Anal. Chem. 87, 11739–11745.
Zhou, M., Liu, S., Jiang, Y., Ma, H., Shi, M., Wang, Q., 2015. Adv. Funct. Mater. 25, 4730–4739.
Zhou, X., Su, F., Lu, H., Senechal-Willis, P., Tian, Y., Johnson, R.H., Meldrum, D.R., 2012. Biomaterials 33, 171–180.
Zhu, D., Jiang, X.X., Zhao, C., Sun, X.L., Zhang, J.R., Zhu, J.J., 2010. Chem. Commun. 46, 5226–5228.
Zhu, D., Li, W., Wen, H.M., Yu, S., Miao, Z.Y., Kang, A., Zhang, A.H., 2015. Biosens. Bioelectron. 74, 1053–1060 2015.
Zhu, D., Li, W., Ma, L., Lei, Y., 2014. RSC Adv. 4, 9372–9378.
Zhu, D., Miao, Z.Y., Hu, Y., Zhang, X.J., 2018. Biosens. Bioelectron. 100, 475–481.
Zhu, H., Fan, J., Du, J., Peng, X., 2016. Acc. Chem. Res. 49, 2115–2126.